The Plant Cell, Vol. 28: 2464–2477, October 2016, www.plantcell.org

A Model of Differential Growth-Guided Apical Hook Formation in Plants

Petra Žádníková,[a,b,1,2] Krzysztof Wabnik,[c,1,3] Anas Abuzeineh,[a,b] Marçal Gallemi,[c] Dominique Van Der Straeten,[d] Richard S. Smith,[e] Dirk Inzé,[a,b] Jiří Friml,[c] Przemysław Prusinkiewicz,[f] and Eva Benková[c,4]

[a] Department of Plant Systems Biology, VIB, Gent 9052, Belgium
[b] Department of Plant Biotechnology and Bioinformatics, Ghent University, Gent 9052, Belgium
[c] Institute of Science and Technology Austria, Klosterneuburg 3400, Austria
[d] Laboratory of Functional Plant Biology, Department of Physiology, Ghent University, Gent 9000, Belgium
[e] Department of Comparative Development and Genetics, Max Planck Institute for Plant Breeding Research, Köln 50829, Germany
[f] Department of Computer Science, University of Calgary, Calgary, Alberta T2N 1N4, Canada

ORCID IDs: 0000-0003-4675-6893 (M.G.); 0000-0002-7755-1420 (D.V.D.S.); 0000-0001-9220-0787 (R.S.S.); 0000-0002-3217-8407 (D.I.); 0000-0002-8302-7596 (J.F.); 0000-0002-8510-9739 (E.B.)

Differential cell growth enables flexible organ bending in the presence of environmental signals such as light or gravity. A prominent example of the developmental processes based on differential cell growth is the formation of the apical hook that protects the fragile shoot apical meristem when it breaks through the soil during germination. Here, we combined in silico and in vivo approaches to identify a minimal mechanism producing auxin gradient-guided differential growth during the establishment of the apical hook in the model plant *Arabidopsis thaliana*. Computer simulation models based on experimental data demonstrate that asymmetric expression of the PIN-FORMED auxin efflux carrier at the concave (inner) versus convex (outer) side of the hook suffices to establish an auxin maximum in the epidermis at the concave side of the apical hook. Furthermore, we propose a mechanism that translates this maximum into differential growth, and thus curvature, of the apical hook. Through a combination of experimental and in silico computational approaches, we have identified the individual contributions of differential cell elongation and proliferation to defining the apical hook and reveal the role of auxin-ethylene crosstalk in balancing these two processes.

INTRODUCTION

Plants have evolved means to protect the fragile shoot apical meristem when growing through the soil toward the surface. Shortly after germination, the hypocotyls bend into hook-shaped structures that shield the apical meristem. The hook that is formed by differential growth via coordinated cell elongation and cell division in the distal part of the hypocotyl is maintained as long as the hypocotyl elongates in the dark and rapidly straightens out after exposure to light (Raz and Ecker, 1999; Raz and Koornneef, 2001; Žádníková et al., 2010).

One of the major regulators of apical hook development is the phytohormone auxin (Abbas et al., 2013; Lehman et al., 1996). Interference with either auxin metabolism or downstream auxin responses severely affects apical hook development. For instance, reduced curvature was observed in the auxin biosynthesis mutant *yucca1* (Zhao et al., 2001), the auxin overproduction mutant *superroot1* (Boerjan et al., 1995), and auxin signaling mutants such as *auxin resistant1* (Leyser et al., 1993) and *non-phototrophic hypocotyl* (Harper et al., 2000). The disruption of apical hook formation by inhibition of auxin transport via pharmacological or genetic manipulations indicates that polar auxin transport is important during apical hook development (Žádníková et al., 2010; Lehman et al., 1996; Schwark and Schierle, 1992; Vandenbussche et al., 2010; Wu et al., 2010). Monitoring auxin responses with the synthetic *DR5* reporter revealed that auxin gradually accumulates at the concave side during hook formation (Žádníková et al., 2010; Vandenbussche et al., 2010). This auxin maximum is maintained in the closed hook and gradually disappears as the hook opens. These remarkable dynamics of auxin distribution rely on tightly controlled polar auxin transport. Based on detailed expression and functional analyses of the AUXIN/AUXIN-LIKE (AUX/LAX) influx (Vandenbussche et al., 2010) and PIN-FORMED (PIN) efflux carriers (Žádníková et al., 2010), it has been proposed that auxin biosynthesized in the cotyledons, shoot apical meristem, and apical zone of the hypocotyl is directed toward the root by the coordinated activities of the influx carrier AUX1 and efflux carriers PIN1 and PIN3 that act in the central cylinder. Subsequently, auxin is laterally redistributed into the endodermis by PIN3 and further through the cortex and the epidermis by AUX1, PIN3, PIN4, and PIN7 (Žádníková et al., 2010; Vandenbussche et al., 2010). Other important players in the control of hook formation are upstream regulators of auxin carrier activity. AUX1 exocytosis to the plasma membrane depends on the activity of the trans-Golgi network-localized ECHIDNA protein

[1] These authors contributed equally to this work.
[2] Current address: Institute of Developmental Genetics, Cluster of Excellence on Plant Sciences, Heinrich-Heine University, 40225 Düsseldorf, Germany.
[3] Current address: University of California, San Diego, Biocircuits Institute, San Diego, CA 92903.
[4] Address correspondence to eva.benkova@ist.ac.at.
The author responsible for distribution of materials integral to the findings presented in this article in accordance with the policy described in the Instructions for Authors (www.plantcell.org) is: Eva Benková (eva.benkova@ist.ac.at).
www.plantcell.org/cgi/doi/10.1105/tpc.15.00569

complex (Boutté et al., 2013), and PIN3 activity during hook formation is dependent on the function of WAG2, a member of the AGC kinase family (Willige et al., 2012).

The auxin responses that direct the hook development are tightly coordinated by crosstalk with other hormonal pathways including that of ethylene. Etiolated *Arabidopsis thaliana* seedlings with either increased ethylene levels or constitutively activated ethylene signaling cascade due to mutations in *ETHYLENE OVERPRODUCER1* or *CONSTITUTIVE TRIPLE RESPONSE1*, respectively, display an exaggerated apical hook (Guzmán and Ecker, 1990; Roman and Ecker, 1995). By contrast, the ethylene-insensitive mutants *ethylene resistant1* (*etr1*) or *ethylene insensitive2* are either hookless or exhibit severe defects in apical hook development (Raz and Ecker, 1999; Guzmán and Ecker, 1990). Although ethylene and auxin can act on downstream target genes in a partially independent manner, they also tend to exhibit crosstalk (Li et al., 2004; Stepanova et al., 2005, 2007). Specifically, ethylene promotes the expression of *TRYPTOPHAN AMINOTRANSFERASE2* (*TAR2*) and thus increases auxin levels in the apical hook (Vandenbussche et al., 2010). Ethylene also influences auxin transport by modulating the expression of several *PIN* genes (Žádníková et al., 2010). Another convergence point of the ethylene and auxin pathways is *HOOKLESS1* (*HLS1*), which encodes a putative *N*-acetyltransferase (Lehman et al., 1996). Ethylene stimulates the transcription of *HLS1*, which in turn inhibits the expression of the *AUXIN RESPONSE FACTOR2* auxin signaling repressor gene, thereby promoting auxin responses (Li et al., 2004).

Although the role of auxin and its differential distribution (the "auxin gradient") in establishing the apical hook development is well recognized, the detailed mechanisms that underlie formation and developmental interpretation of the auxin gradient into differential cell growth are still unclear. Here, we combine experimental and computational methods to investigate the mechanistic basis for the auxin gradient-driven apical hook formation. First, we show that the axial asymmetry of *PIN* expression in the cortex and epidermis plays a crucial role in generating a sharp auxin maximum in the epidermis on the concave hook side. Second, we simulate the effect of auxin on cell elongation and growth dynamics, and demonstrate how the auxin distribution may define apical hook shape. To validate our model predictions, experiments were designed to examine the influence of perturbed auxin distribution, ethylene perception, and cell proliferation on apical hook shape. As a result, we propose that the interplay between the auxin and ethylene signaling pathways coordinates both cell division and differential cell growth for proper hook bending and to fine-tune its curvature.

RESULTS

An Auxin Response Maximum Is Centered at the Concave Apical Hook Side in the Epidermal Cells

The auxin maximum at the concave side of the curvature coordinates the formation of the apical hook (Žádníková et al., 2010; Vandenbussche et al., 2010; Li et al., 2004). However, the precise positioning of this auxin maximum and the mechanistic details of its establishment are not fully understood (Žádníková et al., 2010; Vandenbussche et al., 2010). Previously, PIN3 has been identified as the principal auxin transporter in the apical hook and has been proposed to direct auxin from the central cylinder through the endodermis toward the cortex and epidermal tissue layers (Žádníková et al., 2010). In the cortex and epidermis, PIN3-mediated transport is assisted by PIN4 and PIN7, which exhibit partially overlapping expression patterns. Quantification of the PIN3 and PIN4 accumulation by means of the GFP reporter has revealed that their levels in the cortex cells are higher at the convex than at the concave side of the apical hook (Žádníková et al., 2010; Supplemental Table 1). Hence, we hypothesized that this *PIN3* and *PIN4* expression asymmetry leads to the formation of an auxin maximum on the inner, concave side of the hook (Žádníková et al., 2010).

To test this hypothesis, we developed a computer simulation model of the cross section of the apical hook. The model, based on experimental data for the polar *PIN* expression patterns associated with apical hook formation (Žádníková et al., 2010), operates on a cellular template derived from confocal microscopy images processed with digital segmentation algorithms (MorphoGraphX; http://www.morphographx.org/) (Žádníková et al., 2010; Kierzkowski et al., 2012; Barbier de Reuille et al., 2015) (Supplemental Methods). As the exact mechanism that controls differential *PIN3* and *PIN4* expression (generally referred to *PIN* expression in our model) at the concave and convex hook sides is not known, we assumed that the cell position within the hook cross section was translated by a simple relation into the *PIN* expression rate in the cell (Supplemental Methods; Figure 1A) to reflect in planta observations (Žádníková et al., 2010). Specifically, the location of each cell with respect to the reference position on the concave side of the apical hook determined the level of PIN protein activity, such that the cell's *PIN* expression increased with the distance of the cell from the concave hook side (Supplemental Methods; Figure 1A). In our model, the vascular cylinder serves as a source of auxin that is released with a constant rate (Figure 1A, marked by green asterisk) and subsequently drained by PINs toward the endodermis (Figure 1A). Afterwards, endodermis cells pump auxin toward the cortex (Figure 1A). In the cortex tissues, auxin is redistributed by PINs within the cortex and toward the epidermis (Figure 1A). Finally, auxin is radially transported within the epidermis (Figure 1A). This directionality of auxin flow in our model was inferred from in planta PIN localizations previously reported (Žádníková et al., 2010). In addition to PIN-mediated auxin transport, our model integrates a combined passive and active auxin influx (Figure 1A). The mathematical equations describing the auxin transport are given in the Supplemental Methods.

Proceeding from the available experimental data set (Žádníková et al., 2010), we initially assumed that *PIN3* and *PIN4* were differentially regulated only in the cortex tissues and that the highest expression of these *PIN* genes occurred at the convex hook side. The resulting Model A predicted an auxin maximum in the cortex cells on the concave side of the apical hook (Supplemental Figure 1A). We then tested an alternative scenario, in which the differential PIN (combined PIN4 and PIN7) accumulation was assumed in both the cortex and epidermal cells (Model B). Unlike Model A, Model B predicted auxin accumulation in the epidermis on the concave side of the apical hook (Supplemental Figure 1B). To distinguish the best-fitting model, we monitored the auxin response with the synthetic auxin-responsive promoter *DR5rev*

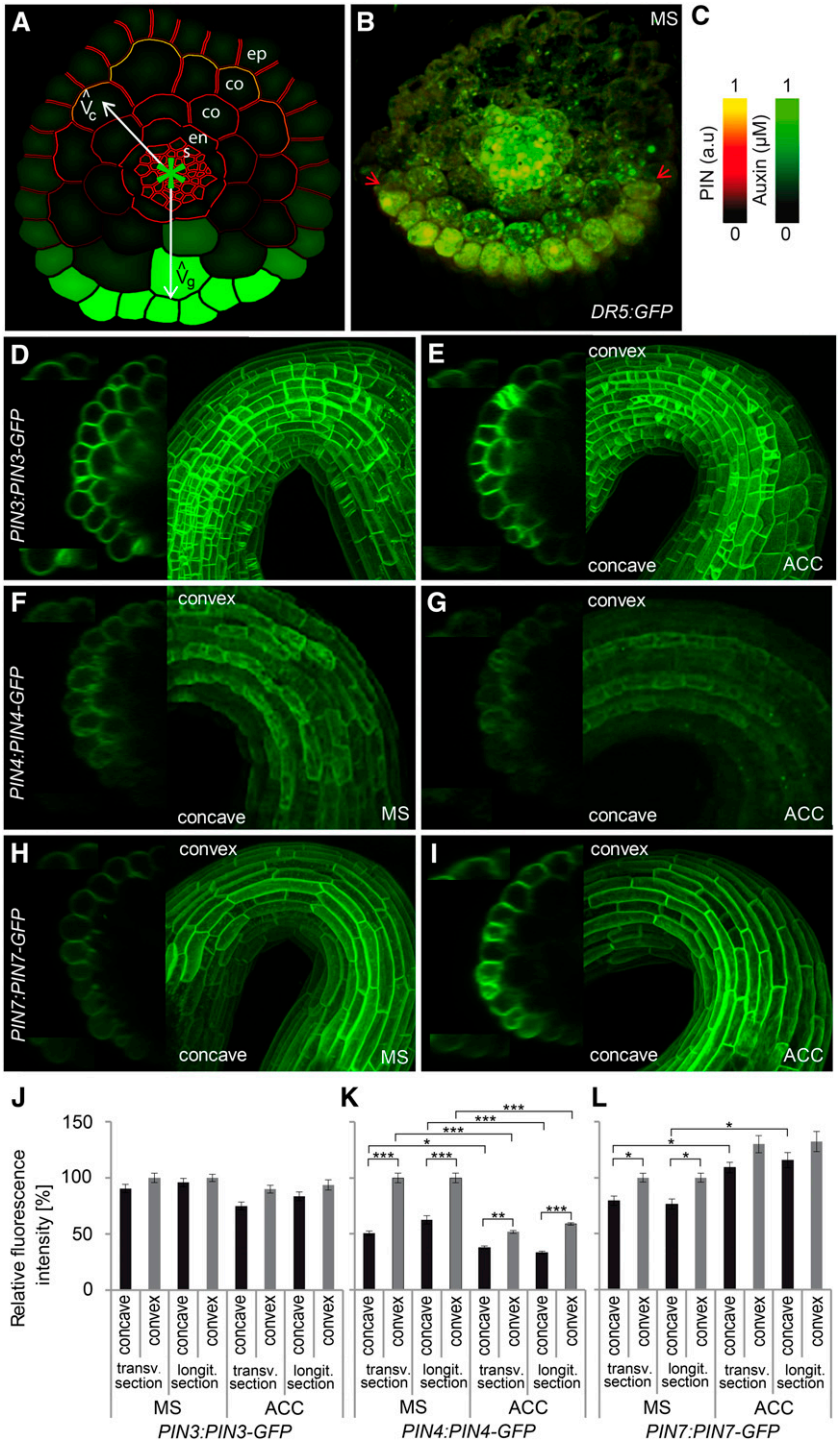

Figure 1. Auxin Accumulation in Epidermal Cells at the Concave Side of the Apical Hook.

(A) Computational model predicting the establishment of the auxin maxima in the epidermal cells at the concave side of an apical hook. *PIN1* is expressed in the vascular tissue (s) marked by a green asterisk (auxin source site), *PIN3* in the endodermis (en), cortex (co), and partially in the epidermis (ep), *PIN4* in the cortex and epidermis (ep), and *PIN7* in the epidermis. The auxin content of the cells is color-coded in green; the cumulative PIN levels (PIN3, PIN4, and PIN7) are presented in red/yellow (heat map). Vector (V_c) points toward the center of the cell mass, while vector (V_g) is reference vector associated with the concave side of the hook. Angle between these two vectors is positively correlated with the *PIN* expression level in the cell.

(B) Transverse section of the apical hook expressing the *DR5rev:GFP* reporter. The auxin response is detected in the epidermal cells at the concave side of the apical hook. Red arrows indicate zone of *DR5rev:GFP*-expressing epidermal cells.

fused to *GFP* (Friml et al., 2003). The transverse sections through the apical hook revealed a strong auxin response in the epidermis and weak activity in a few adjacent cortex cells on the concave hook side (Figure 1B), supporting the predictions of Model B (Figure 1A; Supplemental Figures 1B to 1E). Based on these findings, we concluded that a differential PIN accumulation in both the cortex and epidermal tissues is likely the driving factor that focuses auxin in a few epidermal cells on the concave hook side.

Noteworthy, unlike in the model, high expression of the *DR5rev* auxin reporter in the vascular cylinder could be detected. In the simulation, we assumed that auxin is produced at a constant rate in the vascular cylinder and serves as the auxin supply (marked by green asterisk, Figure 1A). Auxin is then rapidly distributed from the vascular tissues to the outer cell layers. We hypothesize that an elevated *DR5rev* signal detected in the vascular cylinder (Figure 1B) might result from an additional auxin flow from other, not modeled parts of the plant, such as the shoot apical meristem and cotyledons (as proposed in the model by Vandenbussche et al., 2010) or the higher auxin production in the vascular cylinder.

PIN4 and PIN7 Coordinate the Auxin Flux in the Epidermis and Fine-Tune the Formation of the Auxin Maximum

In conjunction with experimental observations, Model B (Figure 1A) suggests that differential expression of *PIN* genes, both in the cortex and epidermis, produces the auxin maximum during apical hook formation. As there were no quantitative data on PIN accumulation in epidermis available, we examined which of the auxin efflux carriers may control the distribution of auxin in the epidermis. Membrane-localized auxin transporters in epidermal cells were quantified on transverse and longitudinal sections of the apical hook acquired by line-scan confocal microscopy and maximal projection of z-stacks images (Figures 1D to 1I; Supplemental Figures 2A and 2B). Despite the enhanced accumulation of PIN3 at the convex side of the cortex (Žádníková et al., 2010; Supplemental Table 1), no significant difference between the two hook sides could be detected in the epidermal cells (Figures 1D and 1J; Supplemental Table 1). By contrast, the PIN4-GFP and PIN7-GFP membrane signals in the epidermis were enhanced at the convex hook side (Figures 1F, 1H, 1K, and 1L; Supplemental Table 1), suggesting that PIN4 and PIN7 promote and coordinate the asymmetric auxin distribution within the epidermis during apical hook formation as predicted by our computer model. In accordance with previous reports, no asymmetry of the AUX1 auxin influx carrier accumulation in epidermal cells at the concave versus convex side of the hook was observed in either transverse or longitudinal sections (Vandenbussche et al., 2010; Supplemental Figures 2A and 2B).

Next, we tested to what extent the spatial differences in the distribution of PIN proteins affects the asymmetric distribution of auxin. The model with reduced PIN accumulation differences (<50%) in the epidermis between concave and convex side of the hook predicted a more diffuse auxin maximum than that of the reference simulation (Supplemental Figures 1F to 1I). To verify this prediction, we examined the auxin distribution in *pin* mutants. The number of epidermal cells with *DR5rev* reporter expression on the transverse hook sections was scored and the proportion was calculated relative to the total number of cells in the epidermis. The transverse hook sections were acquired by either sectioning of fixed samples using vibrating microtome or line-scan confocal microscopy (Figure 2 and Supplemental Figure 3, respectively). In the wild type, on average 44% ± 0.44% and 43.9% ± 0.89% of the epidermal cells had a detectable *DR5rev:GFP* signal in transverse sections when acquired either by sectioning of fixed samples or monitored by line-scan confocal microscopy, respectively (Figures 2B and 2M; Supplemental Figures 3A and 3I). No significant difference in the number of epidermal cells with a *DR5rev:GFP* signal was observed in *pin3* (42.09% ± 0.49% and 44.7% ± 0.99%, respectively) using either of two approaches (Figures 2E and 2M; Supplemental Figures 3C and 3I). By contrast, in both the *pin4* and *pin7* mutants, this number increased significantly to 49.8% ± 0.38% and 50.2% ± 0.97% (Figures 2H and 2M; Supplemental Figures 3E and 3I) and to 54% ± 0.47% and 51.4% ± 1.35% (Figures 2K and 2M; Supplemental Figures 3G and 3I), respectively. These results were quantitatively close to those obtained in the computer model simulations (Figures 2A, 2D, 2G, 2J, and 2M). However, computer model simulations of the *pin4* and *pin7* mutant produced a slightly higher percentage of auxin-containing cells (58%) than those observed in experiments for single *pin4* or *pin7* mutants (Figure 2M), suggesting functional redundancy between the PIN4 and PIN7 proteins. In accordance with the model prediction, the number of epidermal cells exhibiting *DR5rev:GFP* signal in *pin1*$^{+/-}$ *pin3 pin4 pin7* multiple mutant increased to 62.74% ± 1.663% (Supplemental Figures 3K and 3L). Notably, the signal intensity of the *DR5rev:GFP* reporter was reduced in the mutants defective in the auxin transport (Supplemental Figures 3J and 3M). Furthermore, extended in silico analysis was performed to examine the effect of reduced auxin transport rates on the auxin distribution pattern in the apical hook. Simulation of 2-, 5-, and 20-fold reductions of auxin transport rates resulted in gradual diffusion of auxin in the epidermis and weakening of the auxin maximum, thus mimicking the auxin

Figure 1. (continued).

(C) Color coded map for *PIN* expression and auxin levels.

(D) to **(I)** Expression of *PIN:PIN-GFP* reporters in the epidermis of apical hooks grown on either Murashige and Skoog medium (MS) (**[D]**, **[F]**, and **[H]**) or ethylene-supplemented medium (**[E]**, **[G]**, and **[I]**). Membrane PIN-GFP signal detected either at the transverse or longitudinal sections of the apical hook, respectively. Line-scan confocal microscopy and maximal projection of z-stack images used to acquire images. Insets: close-ups of epidermal cells at the convex and concave sides of the apical hook in which membrane PIN-GFP signal was quantified.

(J) to **(L)** PIN-GFP signal quantified at the concave and convex sides of the apical hook epidermal cells in transverse and longitudinal sections of the apical hook, respectively. Significant differences determined by Student's *t* test are indicated as *P < 0.05, **P < 0.001, and ***P < 0.0001; $n = 10$ seedlings, two and five cells analyzed on each side in transverse and longitudinal sections of the apical hook, respectively, at the early maintenance phase 26 h after germination. Error bars represent standard errors.

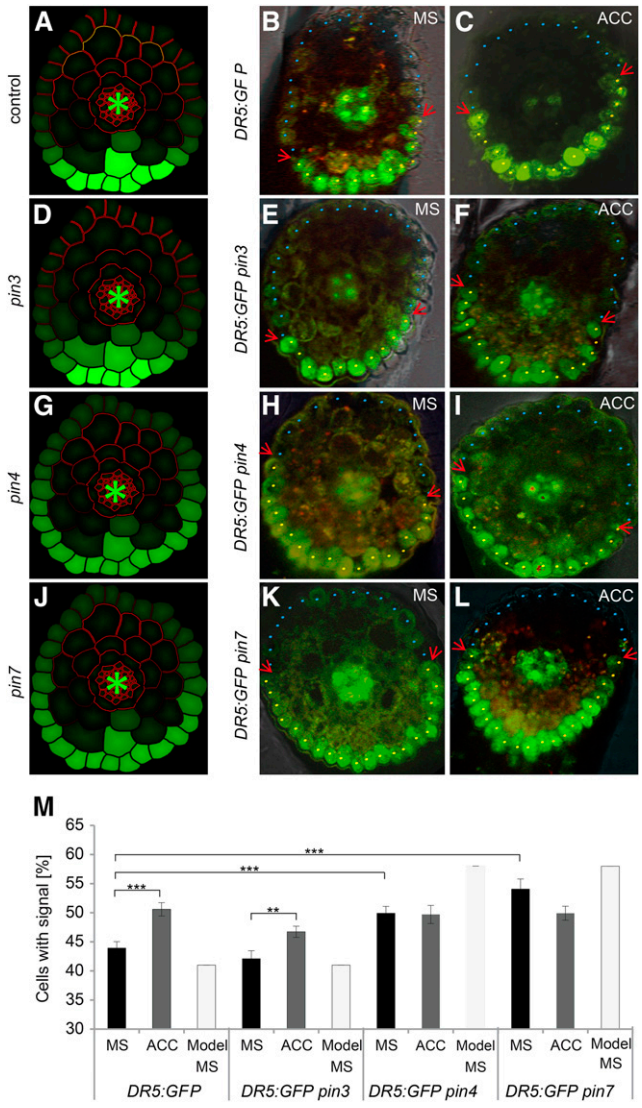

Figure 2. PIN-Controlled Auxin Distribution in Epidermal Cells of the Apical Hook.

(A), **(D)**, **(G)**, and **(J)** Computational model predictions of the auxin distribution in untreated apical hooks of the wild type **(A)**, *pin3* **(D)**, *pin4* **(G)**, and *pin7* **(J)**.

(B), **(C)**, **(E)**, **(F)**, **(H)**, **(I)**, and **(K)** to **(M)** *DR5rev:GFP* expression monitored on transverse sections of untreated (**[B]**, **[E]**, **[H]**, and **[K]**) and ethylene-treated (**[C]**, **[F]**, **[I]**, and **[L]**) apical hooks in the wild-type (**[B]** and **[C]**), *pin3* (**[E]** and **[F]**), *pin4* (**[H]** and **[I]**), and *pin7* (**[K]** and **[L]**). In vivo versus in silico quantifications of the proportion of the *DR5rev*-positive epidermal cells in untreated and ethylene-treated wild-type, *pin3*, *pin4*, and *pin7* mutant plants **(M)**. Yellow and blue dots indicate cells with and without *DR5rev*-reporter signal, respectively. Arrows show boundaries of *DR5rev* signal. Significant differences determined by Student's *t* test are indicated as **P < 0.001 and ***P < 0.0001 (*n* = 10 seedlings at the early maintenance phase, 26 h after germination). Transverse sections acquired by sectioning of fixed samples using vibrating microtome. Error bars represent standard errors.

distribution pattern observed in the *pin* mutant (Supplemental Figures 4A to 4E compared with Supplemental Figures 3K and 3L).

Altogether, these results indicate that PIN3 plays a critical role in supplying auxin from the central cylinder to outer tissues, whereas asymmetric PIN4 and PIN7 activity in the outermost tissues determines the broadness of the radial auxin diffusion in the epidermis. Both experiments and model predictions suggest that the establishment of the confined auxin maximum in the apical hook requires differential asymmetric activity of PIN3 in the cortex and PIN4 and PIN7 in the epidermis.

Ethylene Broadens the Auxin Gradient in the Epidermis of the Apical Hook

In addition to auxin, the plant hormone ethylene plays an important role in the regulation of apical hook development via distinct mechanisms: (1) promotion of auxin biosynthesis by upregulation of *TAR2* expression (Vandenbussche et al., 2010) and (2) modulation of the asymmetric auxin distribution, eventually affecting establishment and positioning of the auxin maximum during apical hook development (Žádníková et al., 2010; Vandenbussche et al., 2010). Defects in ethylene signaling prevent hook formation, whereas increased ethylene levels prolong the developmental hook formation phase and lead to an exaggerated hook phenotype (Žádníková et al., 2010; Vandenbussche et al., 2010; Guzmán and Ecker, 1990; Roman and Ecker, 1995).

To determine the influence of ethylene on the auxin distribution in the apical hook epidermis, we analyzed *DR5rev:GFP*-expressing seedlings that were treated with the ethylene precursor 1-aminocyclopropane-1-carboxylic acid (ACC). The proportion of cells showing *DR5rev* reporter expression in the epidermis was significantly higher (by 6.6% and 8%, when analyzed on the transverse apical hook sections acquired by either vibratome sectioning of fixed samples or by line-scan confocal microscopy, respectively) in ethylene-treated than in untreated apical hooks (Figures 2C and 2M; Supplemental Figures 3B and 3I). Notably, the less confined auxin maxima in ethylene-treated seedlings were reminiscent of those observed in the *pin4* and *pin7* mutants (Figure 2C compared with Figures 2H and 2K; Supplemental Figure 3B compared with Supplemental Figures 3E and 3G) and predicted *pin4* and *pin7* mutant (Figures 2G and 2J). Detailed examination of the ethylene effect on the expression of *PIN3*, *PIN4*, and *PIN7* in the epidermis (Figures 1E, 1G, and 1I to 1L) revealed a dramatic reduction in the PIN4-GFP signal in ethylene-treated apical hooks (Figures 1G and 1K; Supplemental Table 1), in agreement with previous reports using *PIN4:GUS* reporter (Žádníková et al., 2010). By contrast, the PIN7-GFP signal increased on both sides of the apical hook (Figures 1I and 1L; Supplemental Table 1). The PIN3 asymmetry between the convex and concave sides was slightly enhanced by ethylene (Figures 1E and 1J; Supplemental Table 1). Moreover, the expression of *PIN3* as well as *PIN7* was reduced in epidermal cells of the *etr1-3* mutant, thus further supporting a role for the ethylene pathway in maintaining the proper expression of auxin efflux carriers during apical hook development (Supplemental Figures 5A to 5D). These findings are largely in agreement with the previous report (Žádníková et al., 2010) and indicate that the influence of ethylene on auxin transport involves differential regulation of *PIN* expression between the convex and concave sides of the hook.

The combination of PIN3-mediated transport in the inner tissues and asymmetric PIN4 and PIN7 accumulation in the outermost tissues appeared to be central to the auxin transport-driven establishment of the auxin maximum in the epidermis. Therefore, the overall downregulation of *PIN4* along with the disruption of the differential *PIN7* expression by ethylene might contribute to the expansion of the auxin maxima in ethylene-treated hooks. Indeed, treatment of the *pin4* and *pin7* mutants with ethylene did not widen the auxin maximum toward the convex side when compared with untreated hooks (Figures 2I, 2L, and 2M; Supplemental Figures 3F, 3H, and 3I), whereas the *pin3* mutant displayed a more diffused auxin maximum, similar to that of ethylene-treated control plants (Figures 2F and 2M; Supplemental Figures 3D and 3I). This observation suggests that the ethylene-mediated control of *PIN4* and *PIN7* expression is an important mechanism that mediates the polar auxin flux through the epidermis. Notably, although both *pin4* and *pin7* mutants, similarly to ACC-treated seedlings, exhibited diffused expansion of the auxin maximum in the epidermis, the overall amount of auxin in the epidermal tissue of the auxin transport mutant was significantly reduced (Supplemental Figure 3J). Thus, unlike ACC-treated seedlings in which an additional feedback stimulates auxin metabolism and biosynthesis (Vandenbussche et al., 2010), this does not occur in the untreated auxin transport mutants.

A Dynamic Computer Model Integrates the Differential Growth and Graded Cell Proliferation in the Apical Hook Formation

To tackle potential mechanisms of the hook curvature regulation, we developed a dynamic computer model that incorporates differential cell growth and cell proliferation (Figure 3A; Supplemental Figure 6). We used a simplified longitudinal representation of apical hook development by initiating simulations with a few cells (represented by boxes) that mimic the seedling stage (Figure 3A, upper panel). We then defined the "hook zone" by setting distance threshold from the apex (cotyledons) (Figure 3A, lower panel) to enable hook bending as it is observed in planta. For details of the model, refer to Supplemental Methods. This hook zone represents a developmental window where hook bending occurs (Figure 3A, lower panel). In our model, auxin flows from the site of its production (Figure 3A, green bar) toward the exit site (Figure 3A, blue bar). Additionally, auxin is distributed radially within the hook region as well as between convex and concave sides of the hook (Figure 3A, white arrows). *PIN* expression in the hook zone is highest on the outer (convex) side of the hook and lowest at the inner (concave) side, as observed experimentally (Žádníková et al., 2010).

Because auxin negatively influences cell elongation in the hypocotyl (Taiz and Zeiger, 2006), cell elongation rate was inversely correlated with auxin concentrations. Additionally, our model integrates experimental data that include the cell proliferation pattern inferred from the *KNOLLE* (*KN*) reporter (Reichardt et al., 2007), expressed exclusively during cytokinesis (Figure 4A), and the *B-type cyclin 1* (*CYCB1;1*) reporter (Raz and Koorneef, 2001; Ferreira et al., 1994) that marks cells in the G2-to-M transition phase (Supplemental Figure 7A). In agreement with a previous report (Raz and Koorneef, 2001), only cells at a close distance from the cotyledons proliferate rapidly while reaching a given cell area

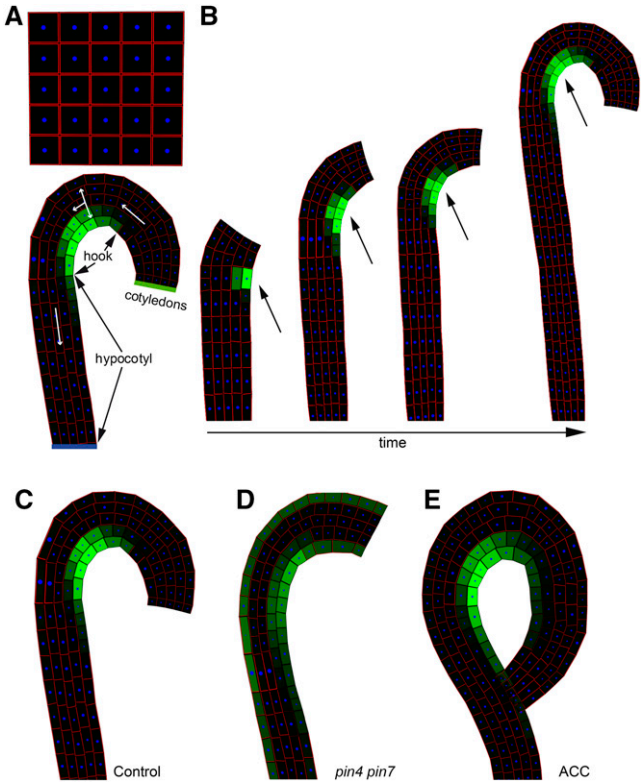

Figure 3. Dynamic Computer Model Suggests a Mechanism for Apical Hook Formation.

(A) Computer-simulated formation of apical hooks started from the early developmental phase, represented by an initial block of cells (denoted as "seedling stage"). The longitudinal hook model was divided into three developmental zones corresponding to the hypocotyl, apical hook, and cotyledons. White arrows depict the preferential directionality of auxin flow from the source (green bar, cotyledons) to the sink (blue bar, basal end of hypocotyl) in the apical hook model. Cells associated with the apical hook zone display strong *PIN* expression on the convex (outer) side of the hook and weak *PIN* expression on the concave (inner) side of the hook as observed experimentally.

(B) Time-lapse computer simulation of "wild-type-like" scenario shows consecutive stages of simulated apical hook formation.

(C) to **(E)** Steady state auxin distribution in the simulated wild-type-like hooks **(C)**, *pin4 pin7* double mutant **(D)**, and simulation integrating the extended zone of rapidly dividing cells (mimicking ethylene treatment, indicated as ACC precursor of ethylene) **(E)**. Color coding for auxin and PIN levels are as in Figure 1C.

threshold (Supplemental Methods). Simulations of growing hypocotyls reproduced a gradual formation of an auxin maximum at the concave side of the apical hook (Figure 3B) similar to predictions of our hook cross-section model (Figure 1A), reproducing that observed in planta (Žádníková et al., 2010). In the model, high and low auxin levels occurred at the concave and convex hook side, respectively, corresponding to the transverse auxin gradient (Figure 3B). Since auxin negatively influences cell elongation in our model, this auxin gradient resulted in differential cell growth and, thereby bending of the apical hook (Figure 3C; Supplemental Figure 6A).

Next, we tested whether the suppressed of the PIN-dependent auxin redistribution affected the curvature of the hook recapitulated by the model. We simulated the multiple *pin4 pin7* mutant by fourfold reducing the overall PIN-mediated auxin transport rate (Figure 3D). This assumption was made to account for the functional redundancy among PIN transporters (Vieten et al., 2005). The model predicted that reduced auxin transport results in a diffused and attenuated auxin maximum at the concave side of the hook, with less pronounced differential cell growth and, thus, impaired apical hook bending (Figure 3D) in agreement with previous observations (Žádníková et al., 2010). In accordance with these findings, either weak or pronounced anisotropy of hook growth integrated in our model led subsequently to under- or overbending of the hook (Supplemental Figures 6B and 6C). Finally, simulations of a near complete lack of auxin transport (a 100-fold reduction in auxin transport rate) resulted in absence of the apical hook and an auxin distribution pattern mimicking that observed in seedlings treated with *N*-(1-naphthyl)phthalamic acid (NPA) inhibitor of auxin transport (Supplemental Figure 4F; Žádníková et al., 2010).

Enhanced Cell Proliferation Promotes Apical Hook Exaggeration

We further examined whether the feedback between the PIN-mediated auxin transport and the auxin-dependent cell growth reproduces the exaggerated hook curvature observed in ethylene-treated seedlings. We first hypothesized that the apical hook exaggeration might require a focused auxin maximum as observed in ethylene-treated seedlings (Vandenbussche et al., 2010). However, our simulations revealed that a more spatially confined auxin maximum is not sufficient to capture the ethylene effect on the hook bending (Supplemental Figure 6D), implying the presence of other mechanisms. Inspection of the cell division pattern by means of the *KN-GFP* or *CYCB1;1:GUS* reporters showed a profound increase in the size of the cell proliferation zone after ethylene treatments (as observed previously; Raz and Koornneef 2001) (Figures 4A, 4B, and 4E; Supplemental Figures 7A, 7B, and 7E). A static integration of this observed enlargement of the cell proliferation zone into the model allowed the reproduction of the exaggerated hook phenotype (Figure 3E; Supplemental Figure 6E).

Following this result, we further examined the role of cell proliferation in apical hook formation. In addition to *KN-GFP* and *CYCB1;1:GUS*, the expression of several other cell division regulatory genes, including *CYCA2;1:GUS*, *CYCA2;2:GUS*, *CYCA2;3:GUS*, *CYCA2;4:GUS* (Vanneste et al., 2011), and *SAMBA:SAMBA-GUS* (Eloy et al., 2012) in the apical hook was detected (Supplemental Figures 8A to 8E) and *CYCA2;2:GUS*, *CYCA2;3:GUS*, and *CYCA2;4:GUS* were upregulated in response to ethylene treatment (Supplemental Figures 8F to 8J). Cell

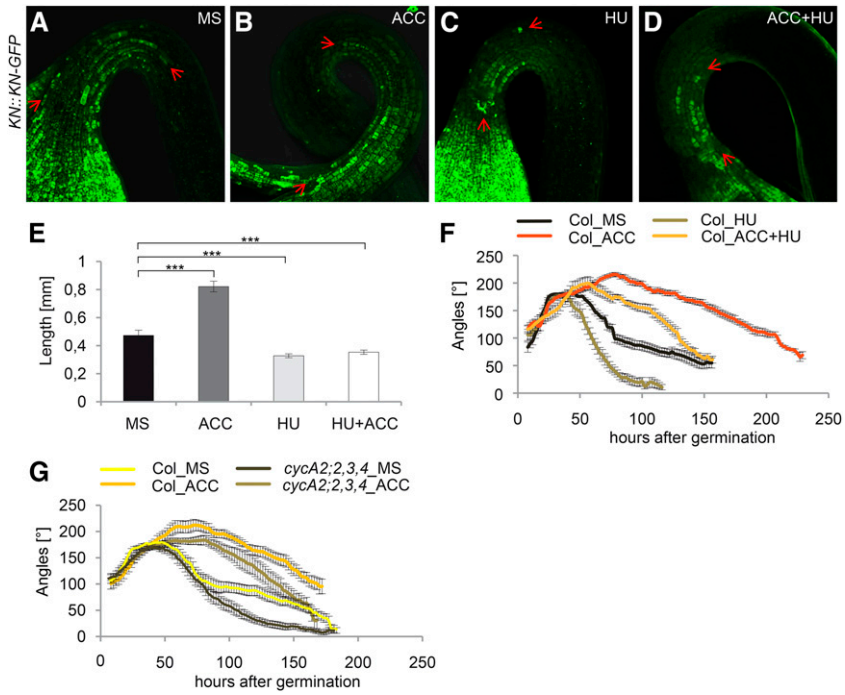

Figure 4. Reduced Cell Proliferation Interferes with Apical Hook Formation.

(A) to **(D)** *KN-GFP* expression during apical hook formation in seedlings treated with MS **(A)**, ACC **(B)** HU **(C)**, and HU+ACC **(D)**. Red arrows mark zone of *KN-GFP* expression.

(E) Quantification of the length of the apical hook zone expressing *KN-GFP*. Significant differences determined by Student's *t* test are indicated as ***P < 0.0001 (*n* = 10 seedlings at the early maintenance phase, 26 h after germination).

(F) and **(G)** Apical hook development in wild-type seedlings treated with HU and ACC+HU **(F)** and *cycA2;2 cycA2;3 cycA2;4* seedlings treated with MS and ACC **(G)** when compared with control (Col). Error bars represent standard errors.

division activity reduced either by a treatment with hydroxyurea (HU) (Figures 4C to 4E; Supplemental Figures 7C to 7E) or due to a lack of *CYCA2;2*, *CYCA2;3*, and *CYCA2;4* expression affected apical hook development. Primarily, neither the seedlings treated with HU nor the multiple loss-of-function mutant *cycA2;2 cycA2;3 cycA3;4* were able to form the ethylene-induced exaggerated hook curvature (Figures 4F and 4G). By contrast, increased cell proliferation caused either by hyperactivity of the GROWTH REGULATING FACTOR5 (Horiguchi et al., 2005) (Figures 5A, 5B, and 5H) or lack of cell cycle repressors, such as SAMBA (Eloy et al., 2012) (Figures 5C, 5D, and 5I), DA1-1, and ENHANCER OF DA1 (EOD1) (Li et al., 2008) promoted exaggerated hook development (Figures 5E to 5G).

Typically, ethylene perception mutants are defective in apical hook development and do not respond to ethylene with hook exaggeration. Hence, we further considered whether some of these defects might result from reduced cell proliferation. Examination of the ethylene receptor mutant *etr1* revealed a dramatically reduced proliferating zone in the presence of ethylene, suggesting that ethylene plays a role in the maintenance of the proper cell proliferation pattern during hook development (Supplemental Figures 9A to 9F). Collectively, our data indicate that the enlargement of the cell proliferating zone presumably enhances the hook flexibility toward deformations, eventually leading to an exaggerated phenotype.

Auxin Coordinates Cell Proliferation and Differential Growth

The combination of experimental and modeling approaches indicated that both the auxin-mediated differential cell growth and cell proliferation (which might be modulated by ethylene) fine-tune the degree of hook bending. To explore in silico the possibility of

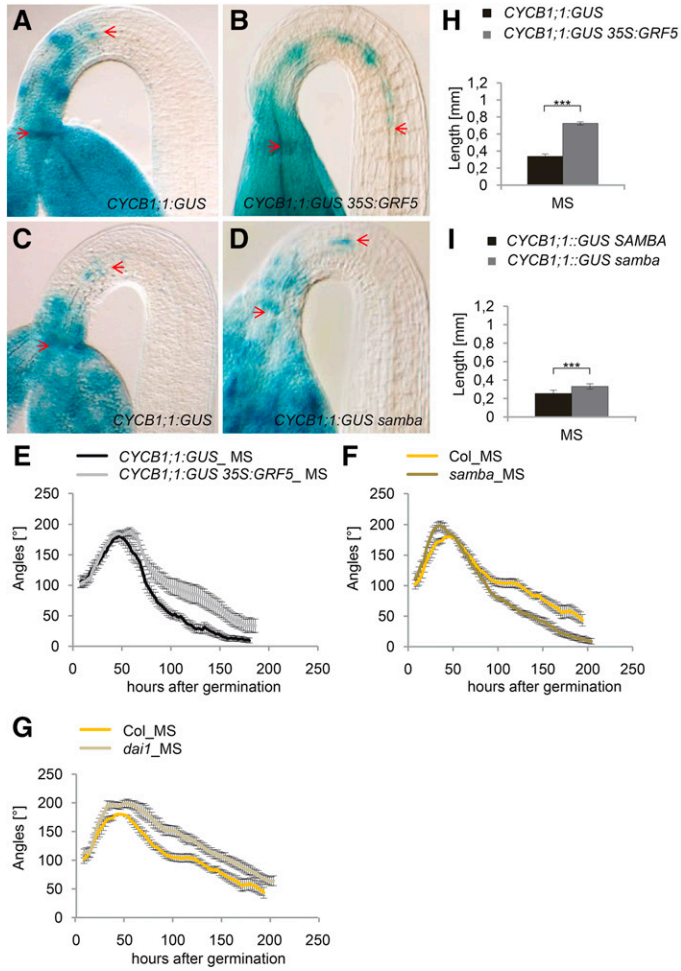

Figure 5. Promoted Cell Proliferation Leads to Apical Hook Exaggeration.

(A) to **(I)** Size of the cell proliferation zones in the *35S:GRF5* line (**[B]**, quantified in **[H]**) and its wild type **(A)** and the *samba* mutant (**[D]**, quantified in **[I]**) and its wild type **(C)** as monitored with *CYC1;1B:GUS*. Significant differences determined by Student's *t* test are indicated as ***P < 0.0001 ($n = 10$ seedlings at the early maintenance phase, 26 h after germination). Red arrows mark zone of *CYC1;1B:GUS* expression.

(E) to **(G)** Kinetics of apical hook development shows exaggeration of the apical hook formation in *35S:GRF5* **(E)**, *samba* **(F)**, and *dai1* **(G)** seedlings. Error bars represent standard errors.

feedback from auxin on the cell proliferation during the apical hook formation, we performed longitudinal hook model simulations (Figure 3A) that integrated the auxin-promoted cell division driving the self-organization of the hook growth in addition to auxin-controlled cell elongation (Supplemental Figure 10). Therefore, we assumed that cells that accumulate auxin levels above a given threshold would proliferate rapidly regardless of their size.

The revisited model faithfully recapitulated the apical hook formation observed in planta (Supplemental Figure 6F). Moreover, our model suggested that ethylene treatments promote either auxin responses or, alternatively, auxin biosynthesis, which is largely in agreement with previous reports on ethylene promoting effect on auxin biosynthesis (Swarup et al., 2007; Vandenbussche et al., 2010; Li et al., 2004). The effect of ethylene preferentially leads to enhanced cell proliferation on the concave hook side (Raz and Koornneef, 2001; see below). In such a scenario, proliferating cells on the concave side are relaxed due to discrete cell division events, whereas cells on the convex side follow rapid outgrowth that results in an exaggerated hook phenotype (Supplemental Figures 6G and 6H).

To further explore these possibilities, we examined mutants defective in auxin transport and signaling. The size of the proliferative zone was reduced significantly in the *pin3* mutant (Figures 6A, 6B, and 6K), previously shown to exhibit significant apical hook development defects (Žádníková et al., 2010) (Figures 6N and 6O) as well as in seedlings treated with the auxin transport inhibitor NPA (Figure 7C and 7H). Similarly, accumulation of the auxin response repressors *solitary root* (*slr*) and *short hypocotyl2-2*

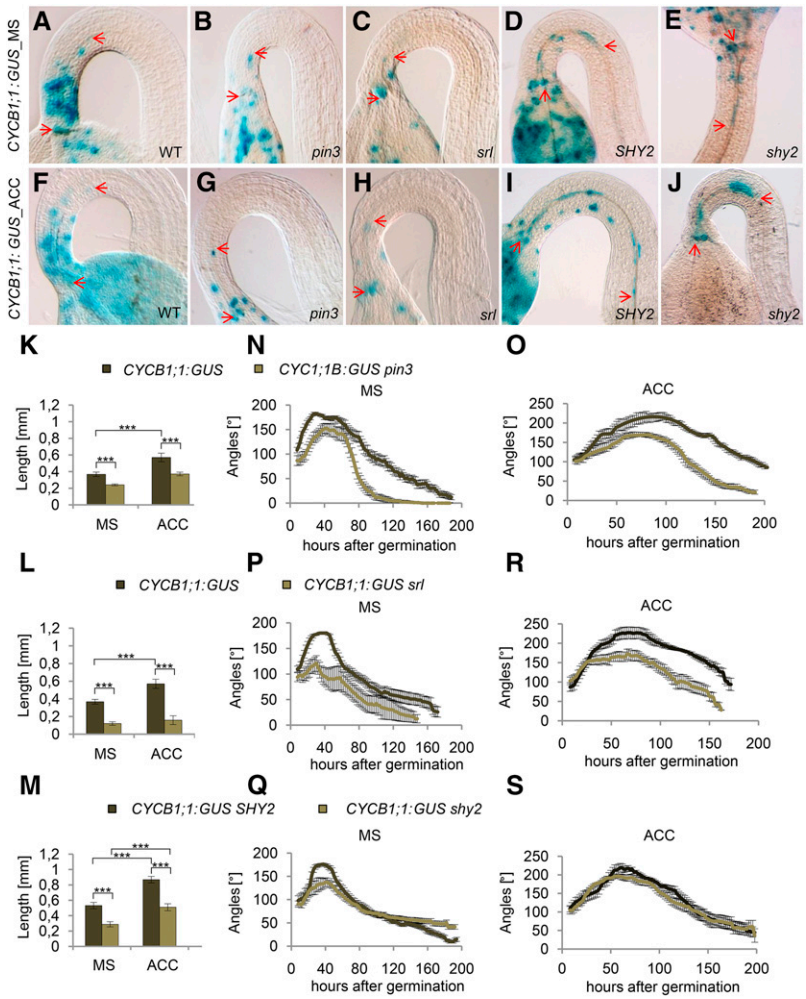

Figure 6. Reduced Cell Proliferation in Auxin-Related Mutants.

(A) to **(M)** Length of the cell proliferation zone in apical hooks of control (**[A]**, **[F]**, and **[K]**), *pin3* (**[B]**, **[G]**, and **[K]**), *slr* (**[C]**, **[H]**, and **[L]**), *SHY2-2* (**[D]**, **[I]**, and **[M]**), and *shy2-2* (**[E]**, **[J]**, and **[M]**) monitored with *CYC1;1B:GUS*. Seedlings germinated on MS medium (**[A]** to **[E]**) and ACC-supplemented medium (**[F]** to **[J]**). Red arrows mark zone of *CYC1;1B:GUS* expression. Significant differences determined by Student's *t* test are indicated as ***$P < 0.0001$ ($n = 10$ seedlings at the early maintenance phase, 26 h after germination).

(N) to **(S)** Apical hook development in *pin3* (**[N]** and **[O]**), *slr* (**[P]** and **[R]**), and *shy2-2* (**[Q]** and **[S]**) on MS (**[N]**, **[P]**, and **[Q]**) and with ACC-supplemented (**[O]**, **[R]**, and **[S]**) medium. Error bars represent standard errors.

(*shy2-2*) in gain-of-function mutants, previously shown to interfere with the apical hook formation (Žádníková et al., 2010) (Figures 6P to 6S), dramatically reduced the size of the cell proliferative zone (Figures 6C to 6E, 6L, and 6M). Furthermore, the cell proliferation defects in the *pin3*, *slr*, and *shy2-2* mutants could not be fully rescued by treatment with ethylene (Figures 6F to 6J and 6K to 6M), indicating that intact auxin activity downstream of ethylene is also required to sustain cell proliferation.

To explore how auxin regulates cell proliferation during apical hook formation, we tested whether auxin responses and cell division patterns could be correlated. Quantification of KN-GFP-positive cells in the apical hook revealed that the proportion of dividing cells at the high auxin level-containing concave hook side was significantly higher than at the convex side (Figures 7A and 7G). Ethylene-treated etiolated seedlings exhibited a larger proliferation zone and the proportion of cells expressing the *KN-GFP* reporter was enhanced at the concave side of the hook (Figures 7B and 7G). By contrast, auxin transport inhibition with NPA impaired the asymmetry of both the auxin response (as previously shown; Žádníková et al., 2010) and cell division patterns (Figures 7C and 7G). Strikingly, the length of the cell proliferation zone detected with the *KN-GFP* reporter correlated with the length of the *DR5rev:GFP*-expressing zone (Figures 7D to 7F and 7H). Altogether, these data indicate that ethylene and auxin jointly coordinate differential cell growth and cell division in a transport-dependent manner during apical hook development.

DISCUSSION

Previous expression and localization studies suggest that an asymmetric distribution of PIN proteins contributes to the establishment of an auxin maximum at the concave side of the hook, thus guiding apical hook formation (Žádníková et al., 2010). However, it was not clear whether such local differences in *PIN* expression were sufficient to direct auxin toward the concave side of the bending hypocotyls, and the precise cellular location of the

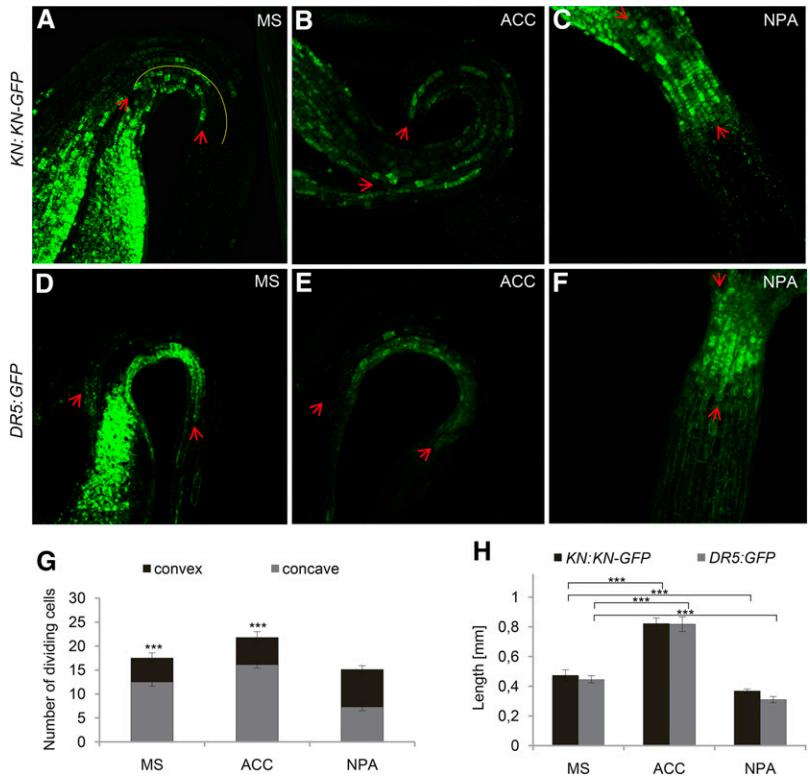

Figure 7. Asymmetric Cell Proliferation Pattern in the Apical Hook Correlates with Auxin Distribution.

(A) to **(C)** Cell proliferation pattern in apical hooks grown on MS **(A)**, ACC **(B)**, and NPA **(C)** monitored with KN-GFP.

(D) to **(F)** Auxin distribution pattern in apical hooks grown on MS **(D)**, ACC **(E)**, and NPA **(F)** monitored with *DR5rev:GFP*. Red arrows mark zone of *GFP* reporter expression.

(G) The number of cells expressing *KN-GFP* at the concave versus the convex side of the apical hooks grown on MS, ACC, and NPA medium. Significant differences in the numbers of cells expressing *KN-GFP* at the concave when compared with convex side determined by Student's *t* test (***P < 0.0001, *n* = 10 seedlings at the early maintenance phase 26 h after germination).

(H) Length of the *KN-GFP* and *DR5rev:GFP* expression zone in apical hooks grown on MS, ACC, and NPA medium. Significant differences of the length of either the *KN-GFP* or *DR5rev:GFP* positive zone when compared with MS grown seedlings (*n* = 10 seedlings at the early maintenance phase 26 h after germination, Student's *t* test ***P < 0.001). Yellow line represents the middle of the apical hook and divides the hook on the convex and concave side. Error bars represent standard errors.

auxin maxima in the hooks was not known. Here, we demonstrated that asymmetric *PIN* expression in both the cortex and epidermal cell layers promotes the transport of auxin toward the concave side of the hypocotyl and that it is sufficient to generate the auxin maximum in the epidermal cells. Application of a computational model was instrumental to dissect the mechanistic basis for the PIN-driven establishment of the local auxin maximum required to determine the curvature of an apical hook. Dynamic computer simulations allowed us to analyze how local perturbations in the auxin transport capacity, such as the lack of differential *PIN* expression or attenuation of PIN activity in the epidermis, might affect the auxin distribution pattern. In agreement with the model's predictions, we observed that attenuated *PIN* expression results in less concentrated auxin maxima that widen toward the convex epidermis side. However, it remains to be investigated which mechanisms determine the initial asymmetry of *PIN* expression and PIN polarities that lead to an auxin maximum on the concave side of the hook.

Our dynamic computer model that integrates auxin-mediated cell elongation and cell proliferation suggests that, while differential cell elongation drives the hook bending, the localized cell proliferation provides means for flexible, growth-induced organ adaptation. This might be particularly important under stress conditions when germinating seedlings must rapidly adapt to environmental changes. Experimental analyses of plants affected in cell proliferation support these predictions. The reduced cell division rate interferes with normal hook development and limits hook bending. By contrast, an enlarged zone of cell proliferation, as revealed by enhanced expression of cell cycle regulators in overexpression lines, correlates with exaggerated apical hook bending. Accordingly, exaggerated apical hooks formed at high ethylene supply exhibited enlarged proliferation zones, indicating that part of the ethylene effect on apical hook development might involve modulation of cell proliferation capacity in the apical zone of the hypocotyl.

Collectively, our modeling and experimental data indicate that the local enlargement of the cell proliferation zone correlates with a higher degree of hook bending. Moreover, the size of the cell proliferation zone was dramatically affected in auxin transport and signaling mutants, suggesting that auxin might contribute to the control of cell proliferation activity during hook development. Our findings suggest that the proportion of cell divisions was higher at the concave side than at the convex side of the hook, thus correlating with auxin accumulation.

Model results, supported by experimental data, demonstrated that ethylene feedback in auxin metabolism (Vandenbussche et al., 2010) and auxin transport might fine-tune the auxin activity and assist in setting the degree of the hook curvature. However, to what extent the ethylene effects on cell proliferation within the apical hook zone are direct or mediated through auxin remains to be explored. Several reports have suggested that part of the ethylene effect involves interaction with auxin biosynthesis (Vandenbussche et al., 2010), auxin signaling (Li et al., 2004), and auxin transport (Vandenbussche et al., 2010; Žádníková et al., 2010); in addition, ethylene effects on other auxin-independent mechanisms that influence cell proliferation cannot be excluded.

Taken together, we identified a putative framework for apical hook formation and the specification of hook curvature, in which an ethylene-auxin crosstalk mechanism instructs differential cell growth and precisely restricts a spatial cell proliferation domain. We propose that hormonal crosstalk confers the regulatory flexibility to modulate polar auxin transport and auxin gradients that effectively feedback on cell growth dynamics and cell division patterning to shape whole-organ curvature and thereby increase the developmental flexibility of a plant to adapt to environmental changes.

METHODS

Plant Material

The transgenic *Arabidopsis thaliana* lines have been described previously: *DR5rev:GFP* (Friml et al., 2003); *PIN3:PIN3-GFP* (Žádníková et al., 2010); *PIN4:PIN4-GFP* and *PIN7:PIN7-GFP* (Blilou et al., 2005) *CYC1;1B:GUS* (Ferreira et al., 1994); *DR5:GUS* (Sabatini et al., 1999); *KN:KN-GFP* (Reichardt et al., 2007); *pin3-4*, *pin4-3*, and *pin7-1* (Žádníková et al., 2010); *DR5rev:GFP pin3-4* (Ding et al., 2011), *DR5rev:GFP pin4-3* (Weijers et al., 2005) and *DR5rev:GFP pin7-1* (Friml et al., 2003); *pin1-1 pin3-5 pin4-3 pin7-1 DR5rev:GFP* (Robert et al., 2013); *CYCA2;1:GUS*, *CYCA2;2:GUS*, *CYCA2;3:GUS*, *CYCA2;4:GUS*, and *cycA2;2 cycA2;3 cycA2;4* (Vanneste et al., 2011); *35S:GRF5* (Horiguchi et al., 2005), *dai1 eod1* (Li et al., 2008), *samba* (Eloy et al., 2012), and *etr1-3* (Guzmán and Ecker, 1990). *PIN3:PIN3-GFP etr1-3* and *PIN7:PIN7-GFP etr1-3* were generated by crosses. The mutants *etr1-3*, *pin3-4*, *shy2-2* (Tian and Reed 1999), *slr* (Fukaki et al., 2002), and *samba* were crossed with *CYC1;1B:GUS* and/or with *DR5rev:GFP*.

Growth Conditions

Seeds were surface sterilized with ethanol, plated on half-strength Murashige and Skoog medium (Duchefa) with 1% sucrose, 0.8% agar, pH 5.7, 5 μM ACC (Sigma-Aldrich), or 5 μM NPA (Duchefa) and 100 μM HU (Sigma-Aldrich), which were added to the media. Seedlings were vernalized for 2 d at 4°C, exposed to light for 12 h at 18°C to synchronize the germination start, and cultivated in the dark at 18°C (Smet et al., 2014). Seedlings 26 h after germination were either imaged by confocal microscopy, stained to detect GUS, or used for transverse sectioning.

Transverse Sectioning of Apical Hook Using Vibrating Microtome

Seedlings 26 h after germination were fixed for 2 h in 3.7% paraformaldehyde (Serva) in MTSB (50 mM PIPES, 5 mM EGTA, and 1 mM $MgSO_4$, pH 6.8) and immobilized in 5% (w/v) low-melting-point agarose (Sigma-Aldrich) in water. The agarose blocks were mounted with agarose onto the stage of a motorized Advance Vibroslice (World Precision Instruments) and 25-μm transverse sections through the apical hook were observed with Zeiss LSM 510 confocal microscope (Carl Zeiss).

Confocal Microscopy

For confocal microscopy imaging, a Zeiss LSM 710 and Zeiss LSM 780 with Zeiss C-Apochromat 63×/1.20 water immersion objective and a Leica TCS SP2 AOBS with HC PL APO 20×/0.70 water immersion objective were used. The GFP signal after a 488-nm argon laser line excitation was detected in the spectral range from 500 to 590 nm for the Zeiss and from 505 to 580 nm for the Leica system.

Optical Transverse Sections of Apical Hook

The confocal microscope Zeiss LSM 780 was used to acquire optical transverse sections of the apical hook. The same seedlings used for

confocal microscopy and further for fluorescence signal quantification were used for optical transverse sections using x-y line scanning in combination with z-stacking through the specimen (typical pixel size: 0.26 μm; thickness of a stack: 20 μm). Fluorescence signals were recorded by a GaAsP point detector and digitalized to build up the confocal x-z image pixel by pixel.

Quantitative Analysis of PIN-GFP and *DR5rev:GFP* Expression

The maximum projection confocal-based pictures were reconstructed with the Zeiss ZEN 2009 software from full z-stacks images of longitudinal whole-mount etiolated seedlings (26-h after germination) taken through the cortex and epidermal layers. These pictures were used for quantitative analysis of fluorescence intensity of the PIN3-GFP, PIN4-GFP, and PIN7-GFP signals. PIN-GFP signal was quantified on transverse membranes (Žádníková et al., 2010) at the convex and concave sides of the apical hooks with ImageJ (NIH; http://rsb.info.nih.gov/ij). At least 10 seedlings were evaluated per treatment and analyzed statistically with GenStat (VSN International, 14th edition).

Quantification of the *DR5rev:GFP* reporter signal intensity was performed on images acquired under strictly identical acquisition parameters for the wild-type Col-0 and the each mutant. Quantification was performed on transverse section images of apical hook acquired by line-scan confocal microscopy (as described above) using ImageJ. A region of interest whose size was kept constant was placed over the concave side of each individual apical hook measured. For each experiment, one epidermal cell positioned in the center of the concave side of the hook was measured. At least 20 seedlings were evaluated per treatment and analyzed statistically with GenStat (VSN International, 14th edition).

Scoring the Proportion of Epidermal Cell Expressing *DR5rev:GFP*

Transverse sections of seedlings carrying *DR5rev:GFP* in the wild-type or mutant background (26 h old) acquired either by sectioning of fixed samples using vibrating microtome or line-scan confocal microscopy were used for scoring the proportion of cells exhibiting *DR5rev:GFP* expression was scored. The number of epidermal cells positive for the GFP signal was scored and the proportion from the total number of epidermal cells in the apical hook was calculated (e.g., 14 cells with a GFP signal out of 29 is equal to 48%). Statistical analysis was done with Genstat (VSN International, 14th edition). The P value for Student's *t* test was 0.01, 0.05, and 0.001.

Quantification of the Length of the Apical Hook Proliferation Zone

Length of the apical hook proliferation zone from shoot apical meristem to the last cell expressing either *KN-GFP* or *CYC1;1B:GUS* was measured. At 26 h after germination, seedlings were measured using ImageJ software (http://rsb.info.nih.gov/ij). At least 10 seedlings were evaluated per treatment and analyzed statistically with Genstat (VSN International, 14th edition).

Real-Time Analysis of Apical Hook Development

Seedling development was recorded at 1-h intervals for 7 d at 18°C with an infrared light source (940 nm LED; Velleman) by a spectrum-enhanced camera (Canon Rebel T2i, 550DH, EF-S 18-55 mm, IS lens kit with built-in clear filter wideband-multicoated and standard Canon accessories) and operated by the EOS utility software. Angles between the hypocotyl axes and cotyledons were measured by ImageJ. Fifteen seedlings with synchronized germination start were processed.

Histochemical Analysis of GUS Activity

Histochemical GUS staining was done as described previously (Žádníková et al., 2010). The staining reaction was performed at 37°C in the dark for 8 h. Seedlings mounted in chloral hydrate (Fluka) were analyzed with a differential interference contrast microscope (BX51 [Olympus] and 10 UPLSAPO objective equipped with a digital CCD camera [2/3-CCD camera], 6.45- to 6.45-μm pixel size, high sensitivity, high resolution, Peltier cooled, dynamic range of 3 to 12 bit). Images were processed with Adobe Illustrator.

Accession Numbers

Sequence data from this article can be found in the Arabidopsis Genome Initiative or GenBank/EMBL databases under the following accession numbers: AT1g70940 (*PIN3*), AT2g01420 (*PIN4*), AT1g23080 (*PIN7*), AT1g73590 (*PIN1*), AT5G25380 (*CYCA2;1*), AT5g11300 (*CYCA2;2*), AT1g15570 (*CYCA2;3*), AT1g80370 (*CYCA2;4*), At1g19270 (*DA1*), At3g63530 (*EOD1*), AT1g32310 (*SAMBA*), AT1g66340 (*ETR1*), AT1g04240 (*SHY2*), AT4g14550 (*SLR*), AT1g04550 (*BDL*), AT4G37490 (*CYC1*), and AT1G08560 (*KN*).

Supplemental Data

Supplemental Figure 1. Simulated *PIN3* expression and auxin distribution in a cross section of the apical hook.

Supplemental Figure 2. Expression of *AUX1:AUX1-YFP* in the epidermis of apical hooks.

Supplemental Figure 3. PIN-controlled auxin distribution in epidermal cells of the apical hook.

Supplemental Figure 4. Simulation of reduced auxin transport mimics auxin distribution observed in auxin transport mutants.

Supplemental Figure 5. Expression of *PIN* auxin efflux transporters in ethylene receptor *etr1-3* mutant.

Supplemental Figure 6. Results of simulated formation of the apical hook.

Supplemental Figure 7. Reduced cell proliferation interferes with apical hook formation.

Supplemental Figure 8. Cell cycle-related gene expression in the apical hook.

Supplemental Figure 9. Reduced proliferation zone in the ethylene receptor mutant.

Supplemental Figure 10. Relation between cell growth rate and auxin concentrations.

Supplemental Table 1. Expression of *PIN:PIN-GFP* reporters in the epidermis and cortex cells of apical hooks.

Supplemental Table 2. Key model parameter summary.

Supplemental Methods. Supporting computational methods.

ACKNOWLEDGMENTS

We thank Martine De Cock and Annick Bleys for help in preparing the manuscript, Daniel Van Damme for sharing material and stimulating discussion, and Rudiger Simon for support during revision of the manuscript. This work was supported by grants from the European Research Council (Starting Independent Research Grant ERC-2007-Stg-207362-HCPO) and the Czech Science Foundation GAČR (GA 13-39982S) to E.B. and Natural Sciences and Engineering Research Council of Canada Discovery Grant 2014-05325 to P.P. K.W. acknowledges funding from a Human Frontier Science Program Long-Term Fellowship (LT-000209-2014). The funders had no role in study design, data collection and analysis, decision to publish, or preparation of the manuscript.

AUTHOR CONTRIBUTIONS

E.B., P.P., P.Z., and K.W. conceived and designed the experiments. P.Z., K.W., R.S.S., A.A., and M.G. performed the experiments. P.Z., K.W., D.V.D.S., R.S.S., D.I., J.F., P.P., and E.B. analyzed the data. P.Z., K.W., P.P., and E.B. wrote the article.

Received July 7, 2015; revised September 8, 2016; accepted October 13, 2016; published October 17, 2016.

REFERENCES

Abbas, M., Alabadí, D., and Blázquez, M.A. (2013). Differential growth at the apical hook: all roads lead to auxin. Front. Plant Sci. **4:** 441.

Barbier de Reuille, P., et al. (2015). MorphoGraphX: A platform for quantifying morphogenesis in 4D. eLife **4:** 05864.

Blilou, I., Xu, J., Wildwater, M., Willemsen, V., Paponov, I., Friml, J., Heidstra, R., Aida, M., Palme, K., and Scheres, B. (2005). The PIN auxin efflux facilitator network controls growth and patterning in *Arabidopsis* roots. Nature **433:** 39–44.

Boerjan, W., Cervera, M.-T., Delarue, M., Beeckman, T., Dewitte, W., Bellini, C., Caboche, M., Van Onckelen, H., Van Montagu, M., and Inzé, D. (1995). *Superroot*, a recessive mutation in Arabidopsis, confers auxin overproduction. Plant Cell **7:** 1405–1419.

Boutté, Y., Jonsson, K., McFarlane, H.E., Johnson, E., Gendre, D., Swarup, R., Friml, J., Samuels, L., Robert, S., and Bhalerao, R.P. (2013). ECHIDNA-mediated post-Golgi trafficking of auxin carriers for differential cell elongation. Proc. Natl. Acad. Sci. USA **110:** 16259–16264.

Ding, Z., Galván-Ampudia, C.S., Demarsy, E., Łangowski, Ł., Kleine-Vehn, J., Fan, Y., Morita, M.T., Tasaka, M., Fankhauser, C., Offringa, R., and Friml, J. (2011). Light-mediated polarization of the PIN3 auxin transporter for the phototropic response in Arabidopsis. Nat. Cell Biol. **13:** 447–452.

Eloy, N.B., et al. (2012). SAMBA, a plant-specific anaphase-promoting complex/cyclosome regulator is involved in early development and A-type cyclin stabilization. Proc. Natl. Acad. Sci. USA **109:** 13853–13858.

Ferreira, P.C.G., Hemerly, A.S., Engler, J.D., van Montagu, M., Engler, G., and Inzé, D. (1994). Developmental expression of the arabidopsis cyclin gene *cyc1At.* Plant Cell **6:** 1763–1774.

Friml, J., Vieten, A., Sauer, M., Weijers, D., Schwarz, H., Hamann, T., Offringa, R., and Jürgens, G. (2003). Efflux-dependent auxin gradients establish the apical-basal axis of Arabidopsis. Nature **426:** 147–153.

Fukaki, H., Tameda, S., Masuda, H., and Tasaka, M. (2002). Lateral root formation is blocked by a gain-of-function mutation in the SOLITARY-ROOT/IAA14 gene of Arabidopsis. Plant J. **29:** 153–168.

Guzmán, P., and Ecker, J.R. (1990). Exploiting the triple response of *Arabidopsis* to identify ethylene-related mutants. Plant Cell **2:** 513–523.

Harper, R.M., Stowe-Evans, E.L., Luesse, D.R., Muto, H., Tatematsu, K., Watahiki, M.K., Yamamoto, K., and Liscum, E. (2000). The NPH4 locus encodes the auxin response factor ARF7, a conditional regulator of differential growth in aerial Arabidopsis tissue. Plant Cell **12:** 757–770.

Horiguchi, G., Kim, G.-T., and Tsukaya, H. (2005). The transcription factor AtGRF5 and the transcription coactivator AN3 regulate cell proliferation in leaf primordia of *Arabidopsis thaliana.* Plant J. **43:** 68–78.

Kierzkowski, D., Nakayama, N., Routier-Kierzkowska, A.-L., Weber, A., Bayer, E., Schorderet, M., Reinhardt, D., Kuhlemeier, C., and Smith, R.S. (2012). Elastic domains regulate growth and organogenesis in the plant shoot apical meristem. Science **335:** 1096–1099.

Lehman, A., Black, R., and Ecker, J.R. (1996). *HOOKLESS1*, an ethylene response gene, is required for differential cell elongation in the Arabidopsis hypocotyl. Cell **85:** 183–194.

Leyser, H.M.O., Lincoln, C.A., Timpte, C., Lammer, D., Turner, J., and Estelle, M. (1993). *Arabidopsis* auxin-resistance gene *AXR1* encodes a protein related to ubiquitin-activating enzyme E1. Nature **364:** 161–164.

Li, H., Johnson, P., Stepanova, A., Alonso, J.M., and Ecker, J.R. (2004). Convergence of signaling pathways in the control of differential cell growth in *Arabidopsis.* Dev. Cell **7:** 193–204.

Li, Y., Zheng, L., Corke, F., Smith, C., and Bevan, M.W. (2008). Control of final seed and organ size by the *DA1* gene family in *Arabidopsis thaliana.* Genes Dev. **22:** 1331–1336.

Raz, V., and Ecker, J.R. (1999). Regulation of differential growth in the apical hook of *Arabidopsis.* Development **126:** 3661–3668.

Raz, V., and Koornneef, M. (2001). Cell division activity during apical hook development. Plant Physiol. **125:** 219–226.

Reichardt, I., Stierhof, Y.-D., Mayer, U., Richter, S., Schwarz, H., Schumacher, K., and Jürgens, G. (2007). Plant cytokinesis requires de novo secretory trafficking but not endocytosis. Curr. Biol. **17:** 2047–2053.

Robert, H.S., Grones, P., Stepanova, A.N., Robles, L.M., Lokerse, A.S., Alonso, J.M., Weijers, D., and Friml, J. (2013). Local auxin sources orient the apical-basal axis in *Arabidopsis* embryos. Curr. Biol. **23:** 2506–2512.

Roman, G., and Ecker, J.R. (1995). Genetic analysis of a seedling stress response to ethylene in Arabidopsis. Philos. Trans. R. Soc. Lond. B Biol. Sci. **350:** 75–81.

Sabatini, S., Beis, D., Wolkenfelt, H., Murfett, J., Guilfoyle, T., Malamy, J., Benfey, P., Leyser, O., Bechtold, N., Weisbeek, P., and Scheres, B. (1999). An auxin-dependent distal organizer of pattern and polarity in the *Arabidopsis* root. Cell **99:** 463–472.

Schwark, A., and Schierle, J. (1992). Interaction of ethylene and auxin in the regulation of hook growth. 1. The role of auxin in different growing regions of the hypocotyl hook of *Phaseolus vulgaris.* J. Plant Physiol. **140:** 562–570.

Smet, D., Žádníková, P., Vandenbussche, F., Benková, E., and Van Der Straeten, D. (2014). Dynamic infrared imaging analysis of apical hook development in Arabidopsis: the case of brassinosteroids. New Phytol. **202:** 1398–1411.

Stepanova, A.N., Hoyt, J.M., Hamilton, A.A., and Alonso, J.M. (2005). A Link between ethylene and auxin uncovered by the characterization of two root-specific ethylene-insensitive mutants in Arabidopsis. Plant Cell **17:** 2230–2242.

Stepanova, A.N., Yun, J., Likhacheva, A.V., and Alonso, J.M. (2007). Multilevel interactions between ethylene and auxin in Arabidopsis roots. Plant Cell **19:** 2169–2185.

Swarup, R., Perry, P., Hagenbeek, D., Van Der Straeten, D., Beemster, G.T., Sandberg, G., Bhalerao, R., Ljung, K., and Bennett, M.J. (2007). Ethylene upregulates auxin biosynthesis in Arabidopsis seedlings to enhance inhibition of root cell elongation. Plant Cell **19:** 2186–2196.

Taiz, L., and Zeiger, E. (2006). Plant Physiology. (Sunderland, MA: Sinauer Associates).

Tian, Q., and Reed, J.W. (1999). Control of auxin-regulated root development by the *Arabidopsis thaliana* SHY2/IAA3 gene. Development **126:** 711–721.

Vandenbussche, F., Petrásek, J., Zádníková, P., Hoyerová, K., Pešek, B., Raz, V., Swarup, R., Bennett, M., Zazímalová, E., Benková, E., and Van Der Straeten, D. (2010). The auxin influx

carriers AUX1 and LAX3 are involved in auxin-ethylene interactions during apical hook development in *Arabidopsis thaliana* seedlings. Development **137:** 597–606.

Vanneste, S., et al. (2011). Developmental regulation of CYCA2s contributes to tissue-specific proliferation in *Arabidopsis.* EMBO J. **30:** 3430–3441.

Vieten, A., Vanneste, S., Wisniewska, J., Benková, E., Benjamins, R., Beeckman, T., Luschnig, C., and Friml, J. (2005). Functional redundancy of PIN proteins is accompanied by auxin-dependent cross-regulation of PIN expression. Development **132:** 4521–4531.

Weijers, D., Sauer, M., Meurette, O., Friml, J., Ljung, K., Sandberg, G., Hooykaas, P., and Offringa, R. (2005). Maintenance of embryonic auxin distribution for apical-basal patterning by PIN-FORMED-dependent auxin transport in Arabidopsis. Plant Cell **17:** 2517–2526.

Willige, B.C., Ogiso-Tanaka, E., Zourelidou, M., and Schwechheimer, C. (2012). WAG2 represses apical hook opening downstream from gibberellin and PHYTOCHROME INTERACTING FACTOR 5. Development **139:** 4020–4028.

Wu, G., Cameron, J.N., Ljung, K., and Spalding, E.P. (2010). A role for ABCB19-mediated polar auxin transport in seedling photomorphogenesis mediated by cryptochrome 1 and phytochrome B. Plant J. **62:** 179–191.

Žádníková, P., et al. (2010). Role of PIN-mediated auxin efflux in apical hook development of *Arabidopsis thaliana.* Development **137:** 607–617.

Zhao, Y., Christensen, S.K., Fankhauser, C., Cashman, J.R., Cohen, J.D., Weigel, D., and Chory, J. (2001). A role for flavin monooxygenase-like enzymes in auxin biosynthesis. Science **291:** 306–309.